Supplementary Information

Comparative Multi-Objective Assessment of Shared and Standalone Rooftop PV-Battery Systems for Energy Autonomy and Infrastructure Efficiency

Nishchaya Kumar Mishra[1], Sameer Patel[1, 2, 3, *]

[1]Department of Civil Engineering, [2]Department of Chemical Engineering, [3]Kiran C. Patel Centre of Sustainable Development, Indian Institute of Technology Gandhinagar, Palaj, Gandhinagar Gujarat 382355, India

Section S1. Household Load Profile, Study Location, and Solar Irradiance

Household energy consumption data for 2018 have been obtained from the eMARC dataset at a 15-minute resolution [1]. The eMARC initiative, led by Prayas Energy Group, collected household electricity consumption data and made it publicly available on the Harvard Dataverse [1]. The dataset contains processed data in three formats: (i) daily energy consumption (kWh) calculated from the cumulative energy consumption data recorded every minute, (ii) 15-minute average power consumption (kW) calculated using one-minute resolution data, and (iii) household information such as city and household type.

The comprehensive eMARC data were further processed to verify the completeness of the energy consumption data (i.e., at least one year of continuous data). For many households, the energy consumption data is missing for durations ranging from a few minutes to many days. Among all the cities, data from Pune, India, was selected for further analysis because the data set corresponding to Pune city has the maximum number of households with at least one year of continuous data. Ultimately, 22 homes were selected, and the energy consumption profiles and statistics for all households are presented in Fig. S1 and Table S1 of Section S1 in the Supplementary Information (SI).

Pune, located in Western India (Fig. S2), receives the maximum and average irradiance of 1063 and 214.46 W/m^2, respectively. For analysis, the solar irradiance received over Pune at 15-minute resolution has been obtained from the National Solar Radiation Database (NSRDB) of the National Renewable Energy Laboratory (NREL), USA [2]. Since NSRDB provides solar irradiance data for 2018 and 2019, the household energy consumption data for 2018 and the corresponding solar irradiance data have been obtained for the investigation carried out in this work. The real-time irradiance data for the study area is shown in Fig. S3 at a 15-minute resolution.

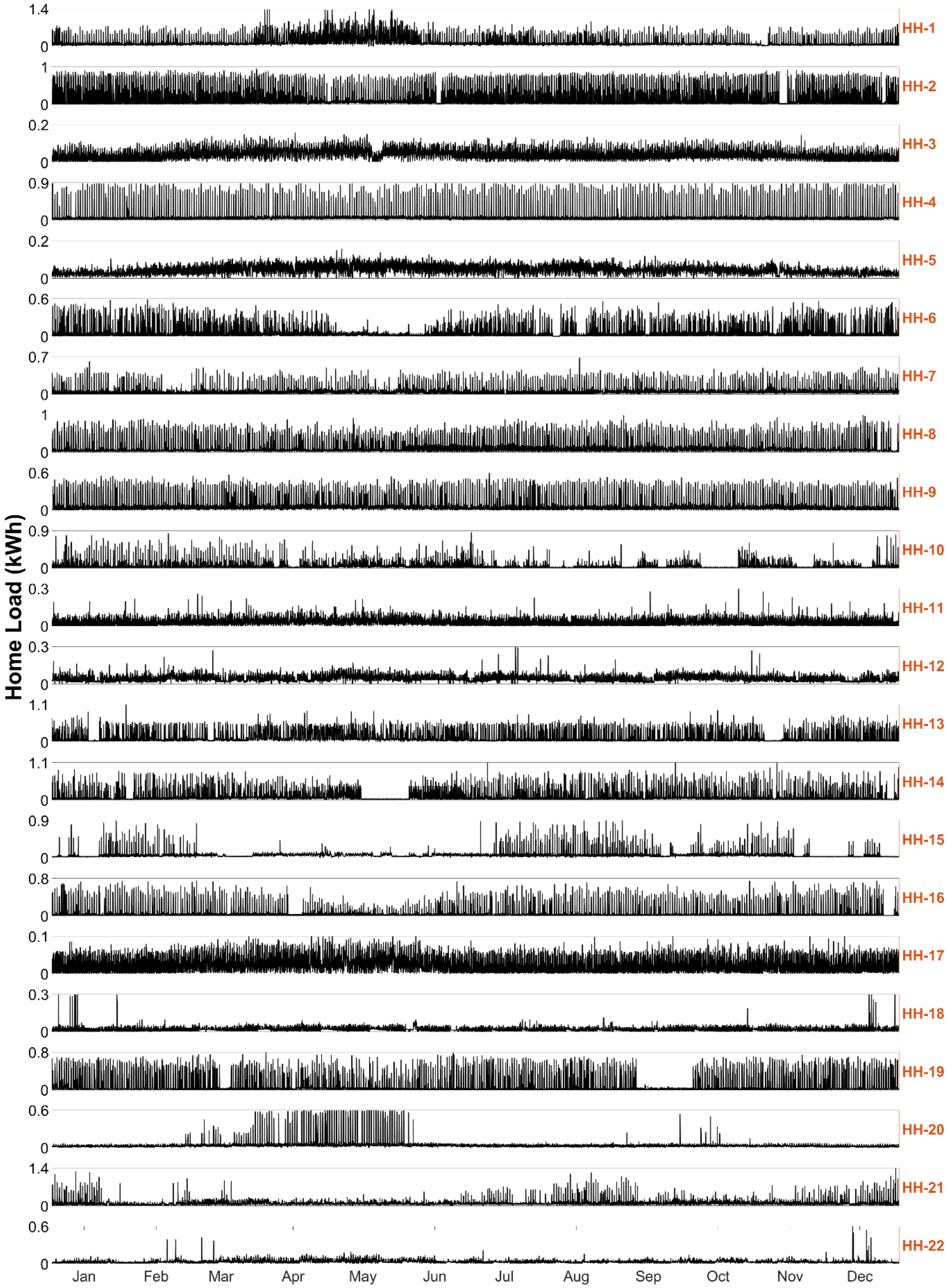

Figure S1. Energy consumption profiles (15-minute resolution) for all households (HH-1 to HH-22) included in the study, as obtained from the eMARC dataset [1].

Table S1. Household characteristics of selected houses. NA: Information Not Available

House No	Household Information		
	No. of rooms	No. of people	Area (in square feet)
HH1	5	4	1100
HH2	3	7	550
HH3	3	4	530
HH4	4	5	700
HH5	3	4	675
HH6	4	3	1000
HH7	5	5	870
HH8	4	4	850
HH9	3	6	600
HH10	5	2	700
HH11	4	5	750
HH12	3	3	945
HH13	4	2	900
HH14	4	4	700
HH15	4	2	700
HH16	3	4	600
HH17	4	3	550
HH18	3	2	575
HH19	3	5	520
HH20	4	3	1000
HH21	NA	NA	NA
HH22	5	4	850

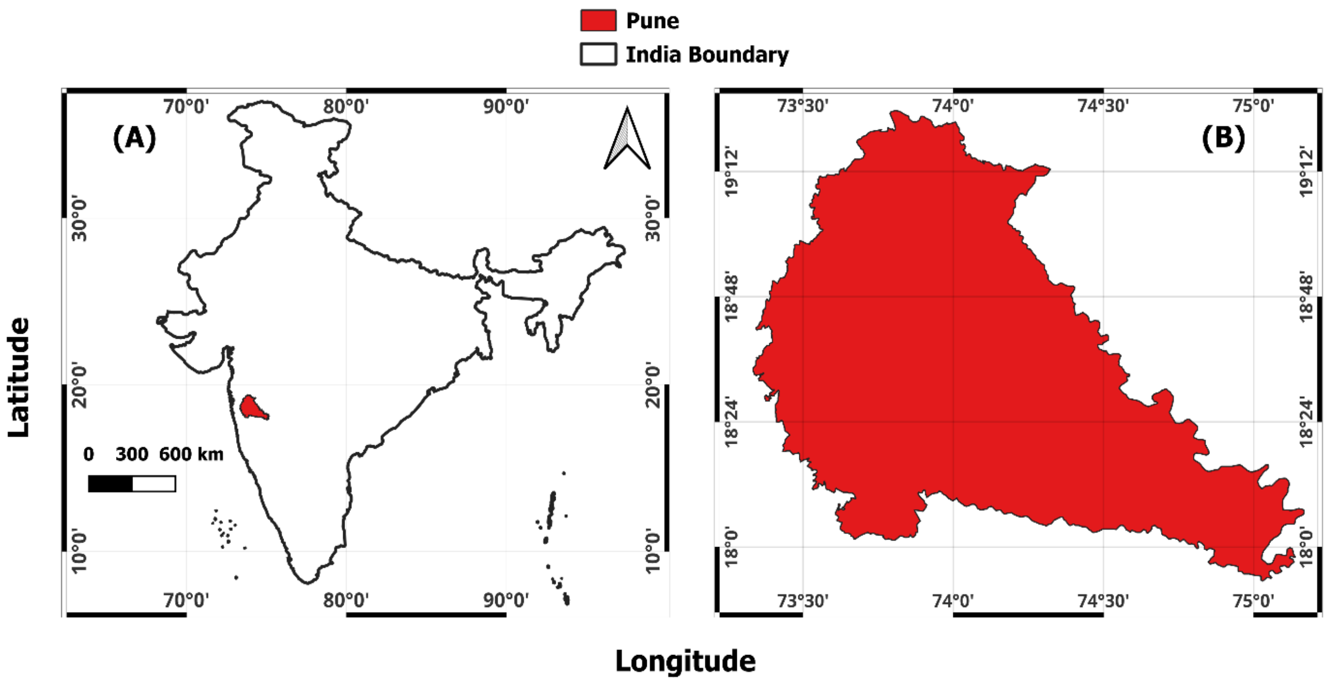

Figure S2. (A) Indian map with international boundary and Pune marked in red, and (B) the administrative boundary of Pune obtained from the Global Administrative Unit Layers (GAUL) [3].

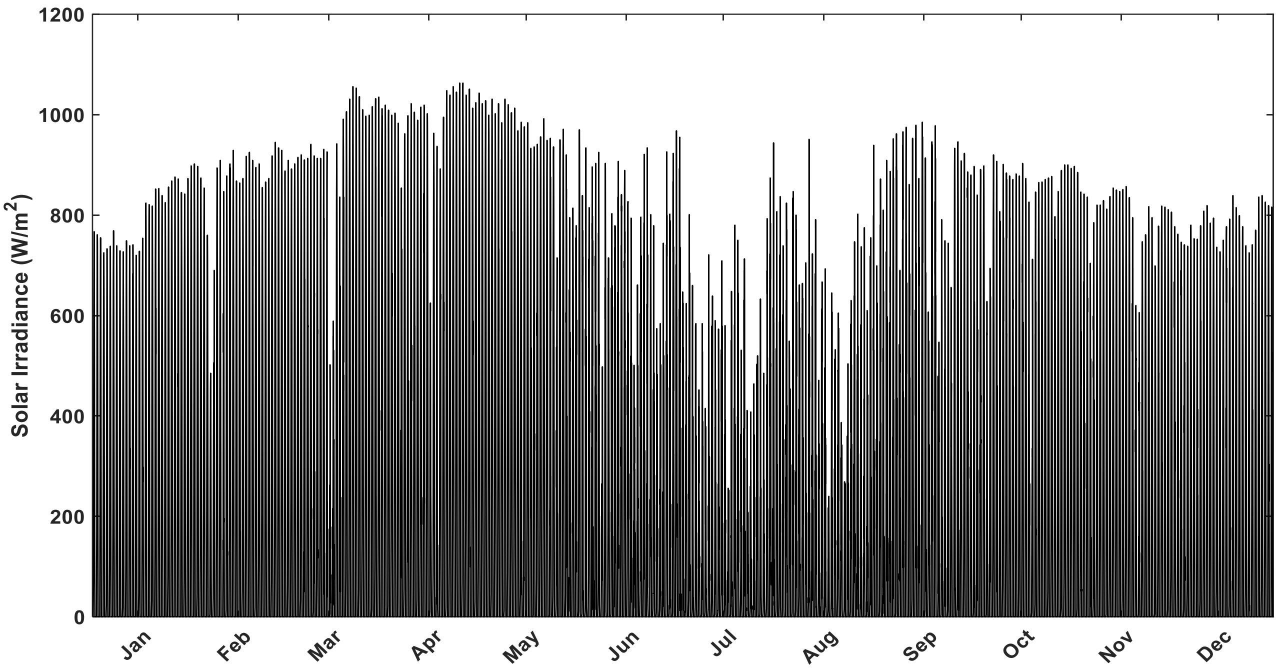

Figure S3. Solar irradiance received over Pune, India, in a typical meteorological year at 15-minute resolution.

Section S2. Battery capacity changes with the battery cycle

Xu et al. [4] proposed a semi-empirical lithium-ion battery degradation model that assessed battery cell life loss from operating profiles. They formulated the model based on fundamental theories of battery degradation and experimental observations from battery aging tests. The battery capacity degradation curve demonstrated in the same study has been adopted, and a model equation has been obtained through curve fitting, as shown in Fig. S4. The obtained equation has been incorporated into the energy management system to model the battery capacity degradation and to determine the number of battery replacements.

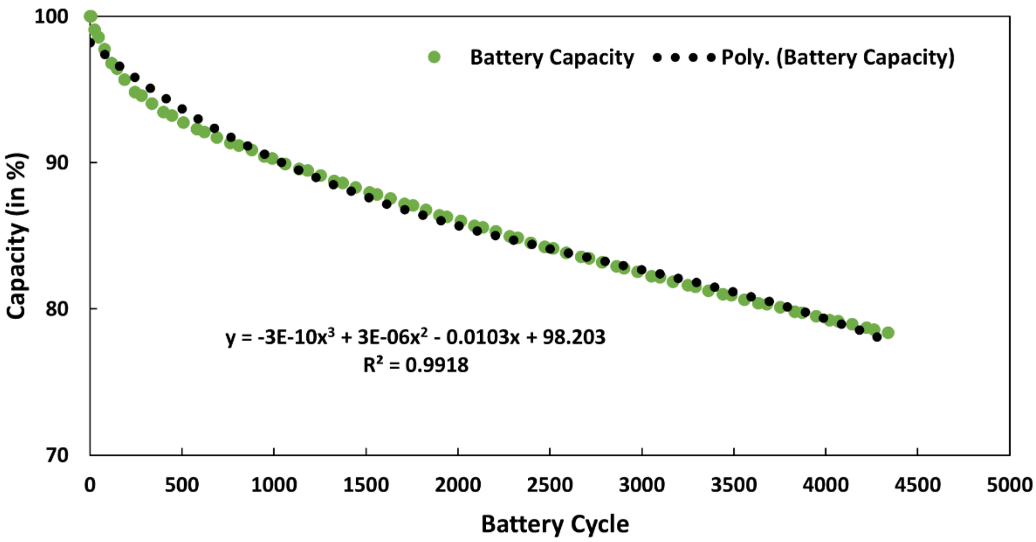

Figure S4. Battery capacity vs battery cycle

One battery cycle is defined as one complete charging and discharging of the battery. In the current algorithm, charging and discharging occur intermittently. Therefore, partial/fractional charge and discharge cycles are calculated and are later used to estimate the total charge cycle (Eq. S1) [5,6].

$$fractional\ charge = \frac{E_{PB}}{B_{Cap}}$$

$$fractional\ discharge = \frac{E_{BH}}{B_{Cap}}$$

$$N_{cycle} = \frac{\sum fractional\ charge + \sum fractional\ discharge}{2}$$

Eq. S1

where, E_{PB} is the energy flow from PV to battery in kWh, E_{BH} is the energy flow from battery to home in kWh, B_{Cap} is the maximum battery storage capacity in kWh, and N_{cycle} is the number of battery storage cycles. It is acknowledged that the simplified model may introduce deviations; however, these assumptions are consistent throughout, and discussions on variations of battery capacity with storage cycles are beyond the scope of this study.

Table S2. Variations (mean ± std) in objectives at different weights assigned to them in the cost function.

Weight Values		Varying Weights							
		W_1		W_2		W_3		W_4	
		Standalone	**Shared**	**Standalone**	**Shared**	**Standalone**	**Shared**	**Standalone**	**Shared**
0.0	**R**	96.6 ± 5.8	67.1 ± 28.9	97.8 ± 3.6	84.9 ± 22.6	98.2 ± 5.4	91.8 ± 23.5	99.8 ± 0.7	95.2 ± 10.9
	CO_2-avoided	55.4 ± 36.9	440.7 ± 415.9	18.5 ± 22.9	97.7 ± 155.7	51.2 ± 40.1	482.1 ± 396.9	79.9 ± 11.8	754.1 ± 219.9
	LC	3.4 ± 2.1	24.8 ± 23.1	1.2 ± 1.3	6.5 ± 8.5	3.1 ± 2.4	27.4 ± 21.6	4.9 ± 0.7	42.4 ± 12.2
	PB	16.3 ± 2.07	12.5 ± 1.6	18.0 ± 2.4	12.6 ± 1.1	17.7 ± 3.1	13.5 ± 1.2	15.4 ± 1.6	13.1 ± 1.1
0.1	**R**	98.9 ± 1.5	93.8 ± 9.9	98.3 ± 3.7	88.0 ± 21.8	98.7 ± 3.2	94.1 ± 16.3	99.9 ± 0.5	96.0 ± 12.4
	CO_2-avoided	55.3 ± 36.5	473.1 ± 400.8	37.3 ± 35.8	278.4 ± 361.9	51.4 ± 38.9	480.1 ± 392.5	72.1 ± 24.3	650.2 ± 340.4
	LC	3.6 ± 2.1	26.7 ± 21.6	2.3 ± 2.1	16.2 ± 19.6	3.1 ± 2.3	27.1 ± 21.1	4.3 ± 1.4	36.1 ± 18.3
	PB	16.2 ± 1.8	12.6 ± 0.8	17.1 ± 2.2	12.6 ± 0.9	16.5 ± 1.9	12.9 ± 0.5	15.4 ± 1.5	12.9 ± 0.7
0.2	**R**	99.3 ± 1.0	98.1 ± 2.5	98.6 ± 3.8	89.5 ± 21.9	98.9 ± 2.1	92.1 ± 17.2	99.7 ± 0.7	96.1 ± 12.1
	CO_2-avoided	54.6 ± 36.9	467.7 ± 396.3	57.3 ± 36.5	426.9 ± 398.9	51.4 ± 38.2	448.8 ± 396.0	63.8 ± 29.7	546.7 ± 381.4
	LC	3.3 ± 2.2	26.5 ± 21.3	3.5 ± 2.1	24.2 ± 21.6	3.1 ± 2.2	25.4 ± 21.4	3.8 ± 1.7	30.6 ± 20.4
	PB	16.3 ± 1.8	12.8 ± 0.4	16.3 ± 1.9	12.7 ± 0.8	16.3 ± 1.7	12.7 ± 0.7	15.7 ± 1.6	12.8 ± 0.7
0.3	**R**	99.7 ± 0.5	99.1 ± 1.7	99.1 ± 3.9	91.8 ± 20.9	99.0 ± 1.7	91.2 ± 17.9	99.5 ± 0.9	93.4 ± 15.8
	CO_2-avoided	54.1 ± 36.7	474.6 ± 393.2	76.9 ± 23.5	673.6 ± 331.0	54.3 ± 36.2	449.2 ± 396.1	54.1 ± 36.3	386.5 ± 389.6
	LC	3.3 ± 2.1	26.9 ± 21.1	4.6 ± 1.4	37.4 ± 17.9	3.3 ± 2.1	25.4 ± 21.4	3.3 ± 2.1	21.9 ± 20.9
	PB	16.3 ± 1.9	12.9 ± 0.3	15.4 ± 1.4	12.9 ± 0.7	16.0 ± 1.4	12.6 ± 0.7	16.2 ± 1.9	12.7 ± 0.7
0.4	**R**	99.8 ± 0.3	99.7 ± 0.4	99.9 ± 0.1	95.7 ± 17.0	99.1 ± 1.6	91.2 ± 17.7	99.1 ± 1.2	89.6 ± 19.5
	CO_2-avoided	53.6 ± 36.7	473.7 ± 386.5	84.1 ± 0.0	808.3 ± 163.9	58.3 ± 33.7	492.4 ± 393.2	38.5 ± 36.7	304.1 ± 374.3
	LC	3.3 ± 2.1	26.9 ± 20.8	5.0 ± 0.0	44.7 ± 9.0	3.5 ± 1.9	27.7 ± 21.3	2.4 ± 2.1	17.5 ± 20.1
	PB	16.4 ± 2.1	13.0 ± 0.0	15.0 ± 0.1	13.1 ± 0.4	15.7 ± 1.1	12.6 ± 0.7	16.9 ± 2.1	12.5 ± 0.8
0.5	**R**	99.9 ± 0.2	99.8 ± 0.2	99.9 ± 0.1	98.7 ± 3.9	99.2 ± 1.3	88.4 ± 19.7	98.5 ± 1.6	86.5 ± 21.7
	CO_2-avoided	55.7 ± 35.9	481.4 ± 384.3	84.1 ± 0.0	840.5 ± 0.1	59.2 ± 32.8	487.0 ± 396.4	27.4 ± 36.7	160.3 ± 285.0
	LC	3.4 ± 2.1	27.3 ± 20.6	5.0 ± 0.0	46.5 ± 0.3	3.6 ± 1.9	27.4 ± 21.5	1.7 ± 2.1	9.8 ± 15.3
	PB	16.4 ± 2.2	13.0 ± 0.0	15.0 ± 0.2	13.0 ± 0.0	15.6 ± 0.9	12.4 ± 0.8	17.7 ± 2.1	12.4 ± 0.9
0.6	**R**	99.9 ± 0.1	99.9 ± 0.2	99.9 ± 0.1	98.3 ± 4.7	99.2 ± 1.3	88.1 ± 19.5	97.1 ± 2.3	76.4 ± 28.8
	CO_2-avoided	52.1 ± 36.7	491.6 ± 384.4	84.1 ± 0.0	840.5 ± 0.1	59.5 ± 31.0	504.7 ± 394.3	8.6 ± 20.9	35.3 ± 16.6
	LC	3.2 ± 2.1	27.9 ± 20.6	5.0 ± 0.0	46.5 ± 0.3	3.6 ± 1.8	28.3 ± 21.4	0.6 ± 1.2	2.9 ± 1.4
	PB	16.7 ± 2.5	13.1 ± 0.3	15.2 ± 0.2	13.0 ± 0.0	15.5 ± 0.8	12.4 ± 0.8	18.9 ± 1.4	12.5 ± 1.1
0.7	**R**	99.9 ± 0.1	99.9 ± 0.2	99.9 ± 0.2	96.6 ± 7.1	98.9 ± 1.3	76.4 ± 24.2	94.0 ± 6.2	71.8 ± 31.3
	CO_2-avoided	41.4 ± 40.9	411.6 ± 384.9	84.1 ± 0.0	840.5 ± 0.2	58.8 ± 29.6	379.7 ± 431.5	2.5 ± 0.5	30.9 ± 15.7
	LC	2.6 ± 2.4	23.7 ± 20.7	5.0 ± 0.0	46.6 ± 0.3	3.6 ± 1.7	21.6 ± 23.7	0.2 ± 0.0	2.7 ± 1.4
	PB	18.0 ± 3.2	13.3 ± 0.5	15.1 ± 0.3	13.0 ± 0.0	15.4 ± 0.7	12.0 ± 1.0	19.5 ± 0.9	12.6 ± 1.3

0.8	**R**	99.9 ± 0.1	99.9 ± 0.1	99.9 ± 0.2	96.6 ± 7.2	99.2 ± 1.3	74.1 ± 22.0	91.3 ± 7.7	62.9 ± 33.1
	CO_2-avoided	55.4 ± 38.3	540.7 ± 375.6	84.1 ± 0.0	840.5 ± 0.2	65.9 ± 24.3	305.7 ± 414.8	2.1 ± 0.5	24.3 ± 14.1
	LC	3.4 ± 2.2	30.7 ± 20.1	5.0 ± 0.0	46.6 ± 0.3	4.0 ± 1.4	17.5 ± 22.8	0.2 ± 0.0	2.2 ± 1.3
	PB	16.9 ± 3.1	13.3 ± 0.8	15.1 ± 0.3	13.0 ± 0.0	15.2 ± 0.4	11.8 ± 0.9	19.9 ± 0.9	12.8 ± 1.7
0.9	**R**	99.9 ± 0.0	99.9 ± 0.0	99.8 ± 0.2	93.6 ± 10.0	98.9 ± 1.2	65.3 ± 18.9	85.5 ± 8.8	44.2 ± 41.6
	CO_2-avoided	51.4 ± 42.2	494.9 ± 391.2	84.1 ± 0.0	840.6 ± 0.3	66.8 ± 16.0	296.7 ± 471.4	1.6 ± 0.4	14.8 ± 14.9
	LC	3.2 ± 2.5	28.4 ± 20.8	5.1 ± 0.0	46.7 ± 0.3	4.0 ± 0.9	16.9 ± 25.9	0.2 ± 0.0	1.5 ± 1.5
	PB	18.1 ± 4.6	13.7 ± 1.1	15.3 ± 0.4	13.0 ± 0.0	15.0 ± 0.0	11.7 ± 1.1	20.4 ± 0.5	14.0 ± 1.0

R is PV reliance in %, CO_2-avoided is total carbon emissions avoided in tonnes CO_2, LC is lifetime cost (x 10^4USD), and PB is payback period in years. All values presented here are mean ± std.

Section S3. Principal component analysis (PCA), k-means clustering, and optimal score function

To identify the governing parameters and explain the differences between individual- and community-scale PV-battery systems, a principal component analysis (PCA) was performed using the normalized percentage changes in panel area, battery storage, PV reliance, lifetime cost, and payback period between the two configurations. The first three principal components (PC1, PC2, and PC3) explained 57.4%, 29.5%, and 10.6% of the total variance, respectively, collectively accounting for approximately 97.5% of the variability in the optimization space. The coefficients of PCs corresponding to the individual change term are presented in Table S3.

Table S3. Coefficients of principal components corresponding to individual change terms

	PC1	PC2	PC3	PC4	PC5
Δpanel	0.557	0.027	-0.450	-0.046	-0.696
Δbattery	0.457	-0.363	0.555	0.591	-0.046
Δreliance	0.396	0.484	0.564	-0.539	0.007
Δcost	0.561	0.064	-0.411	0.048	0.714
Δpayback	-0.096	0.793	-0.041	0.597	-0.059

Based on the dominant PCA trends, PC1, PC2, and PC3 can be expressed as linear functions of different terms (see Eqs. S2, S3, and S4).

$$PC1 = 0.557\,\Delta panel + 0.457\,\Delta battery + 0.396\,\Delta reliance + 0.561\,\Delta cost - 0.096\,\Delta payback$$

Eq. S2

$$PC2 = 0.027\,\Delta panel - 0.363\,\Delta battery + 0.484\,\Delta reliance + 0.064\,\Delta cost + 0.793\,\Delta payback$$

Eq. S3

$$PC3 = -0.450\,\Delta panel + 0.555\,\Delta battery + 0.564\,\Delta reliance - 0.411\,\Delta cost - 0.041\,\Delta payback$$

Eq. S4

Based on these dominant PCA trends, an optimal-score function was formulated as:

$$Optimal\ Score = 0.5\,PC1 - 0.4\,PC2 - 0.1\,|PC3|$$

Eq. S5

The positive contribution of PC1 rewards technically strong solutions with higher renewable-energy penetration and improved infrastructure deployment. In contrast, PC2 is penalized because larger values correspond to economically unfavorable solutions characterized by longer payback periods. The absolute value of PC3 was used to penalize large deviations in either direction, ensuring that highly unbalanced solutions are assigned lower rankings irrespective of the sign of PC3.

Here, both k-means clustering and the optimal-score analysis are used because they serve two complementary purposes in interpreting the multi-objective optimization space. The k-means clustering identifies naturally occurring groups of solutions with similar characteristics in the reduced PCA space. Since the optimization generates a large number of solutions corresponding to different objective-weight combinations, clustering helps classify these solutions into distinct behavioral regimes or trade-off categories. This enables identification of groups of solutions exhibiting similar balances between PV reliance, storage requirements, cost, and payback characteristics without imposing any prior preference structure. Therefore, clustering provides an unsupervised understanding of the structure and diversity of the solution space. In contrast, the optimal score is used to rank and prioritize solutions according to the desired optimization objectives. While clustering identifies groups of similar solutions, it does not indicate which solutions are preferable. The optimal-score formulation combines the dominant principal components with selected weights to quantify the relative desirability of each solution. This allows identification of high-performing solutions that simultaneously balance technical performance and economic feasibility. Thus, clustering is used to understand the organization and dominant patterns within the solution space, whereas the optimal score is used to evaluate and rank solutions according to the preferred optimization criteria. Together, they provide both qualitative classification and quantitative prioritization of the optimization outcomes.

References

[1] Processed data - Monitoring and Analysis of Residential Electricity Consumption (eMARC) n.d. https://dataverse.harvard.edu/dataset.xhtml?persistentId=doi:10.7910/DVN/YJ5SP1 (accessed February 5, 2025).

[2] NSRDB n.d. https://nsrdb.nrel.gov/data-viewer (accessed February 5, 2025).

[3] FAO GAUL: Global Administrative Unit Layers 2015, First-Level Administrative Units | Earth Engine Data Catalog | Google for Developers n.d. https://developers.google.com/earth-engine/datasets/catalog/FAO_GAUL_2015_level1 (accessed February 5, 2025).

[4] Xu B, Oudalov A, Ulbig A, Andersson G, Kirschen DS. Modeling of lithium-ion battery degradation for cell life assessment. IEEE Trans Smart Grid 2018;9:1131–40. https://doi.org/10.1109/TSG.2016.2578950.

[5] Gundogdu B, Gladwin DT. A Fast Battery Cycle Counting Method for Grid-Tied Battery Energy Storage System Subjected to Microcycles. IEECON 2018 - 6th International Electrical Engineering Congress 2018. https://doi.org/10.1109/IEECON.2018.8712263.

[6] Soto A, Berrueta A, Mateos M, Sanchis P, Ursúa A. Impact of micro-cycles on the lifetime of lithium-ion batteries: An experimental study. J Energy Storage 2022;55:105343. https://doi.org/10.1016/J.EST.2022.105343.